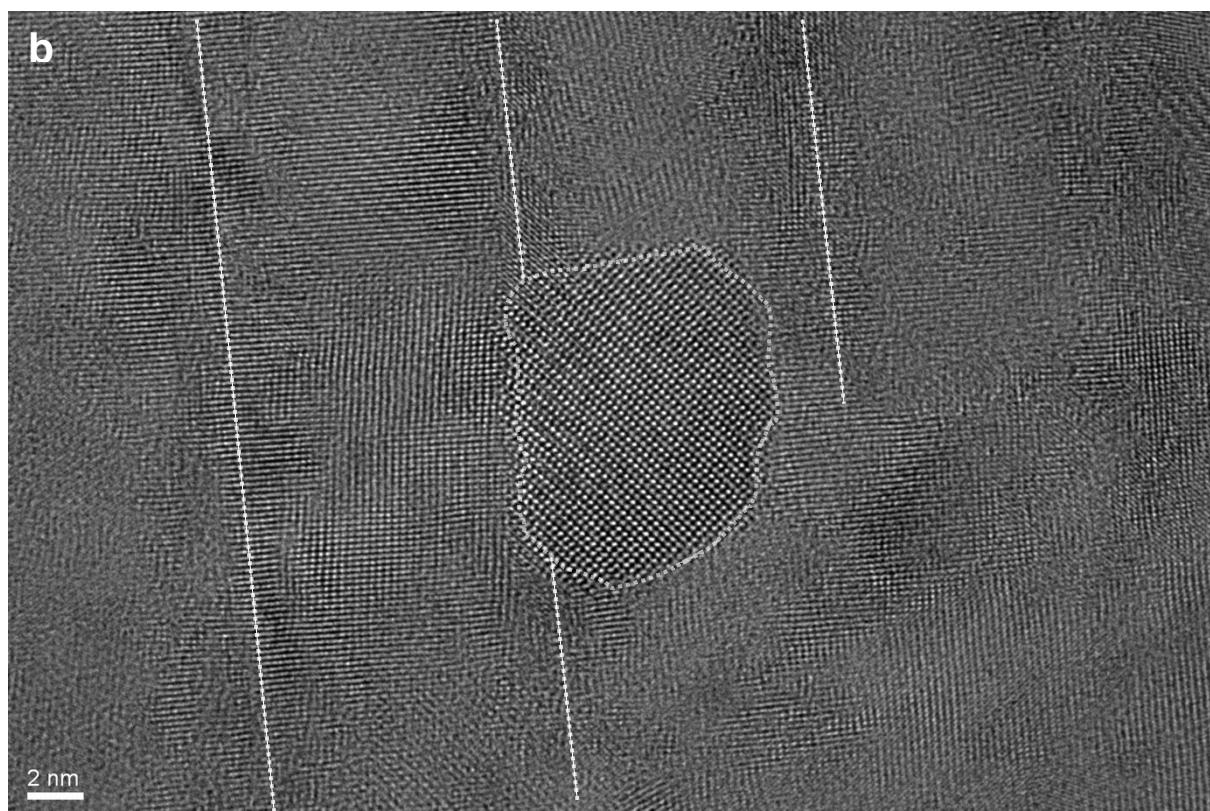
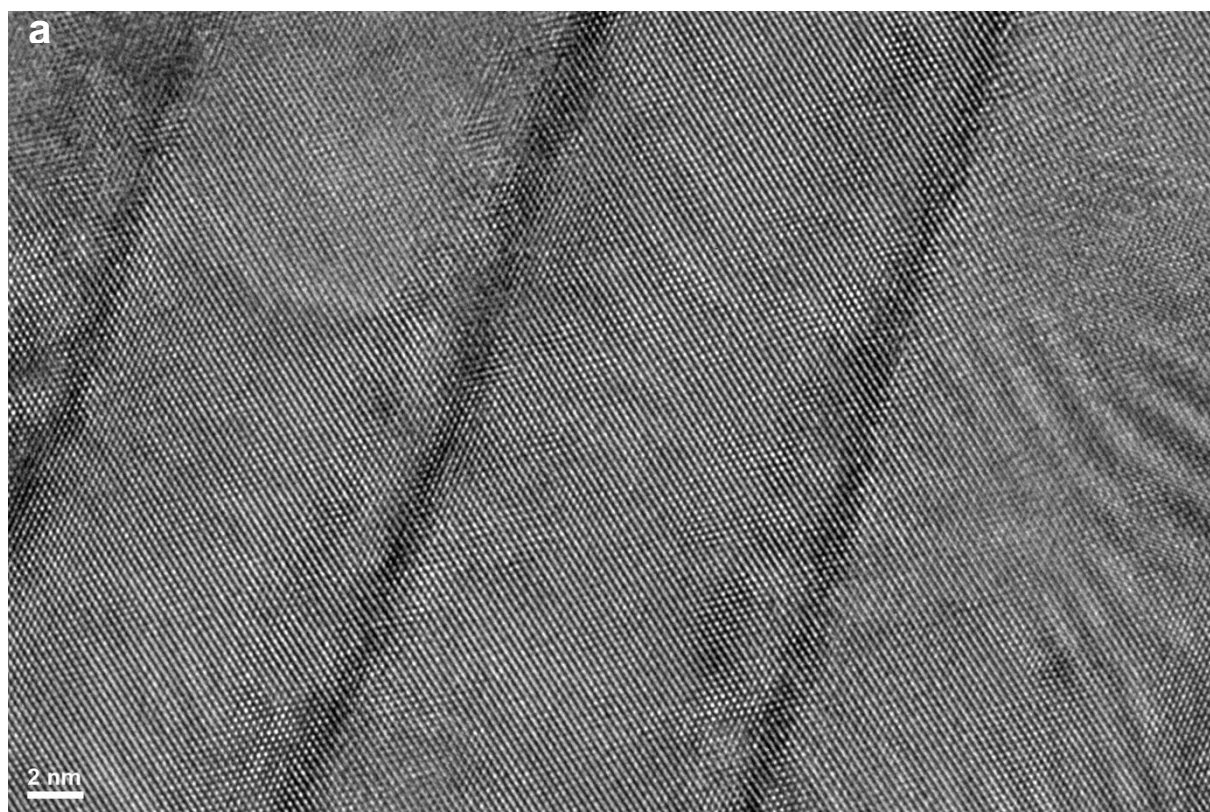
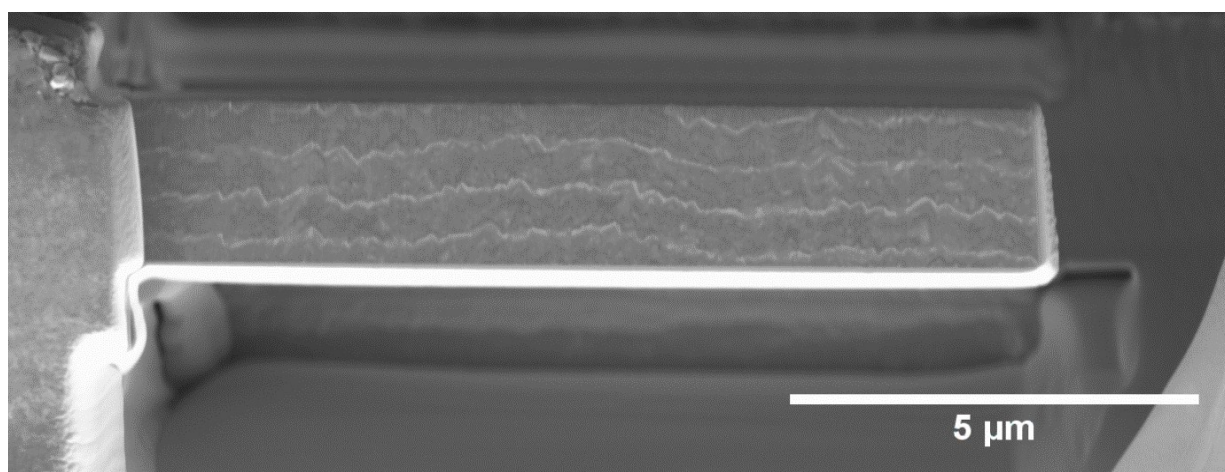


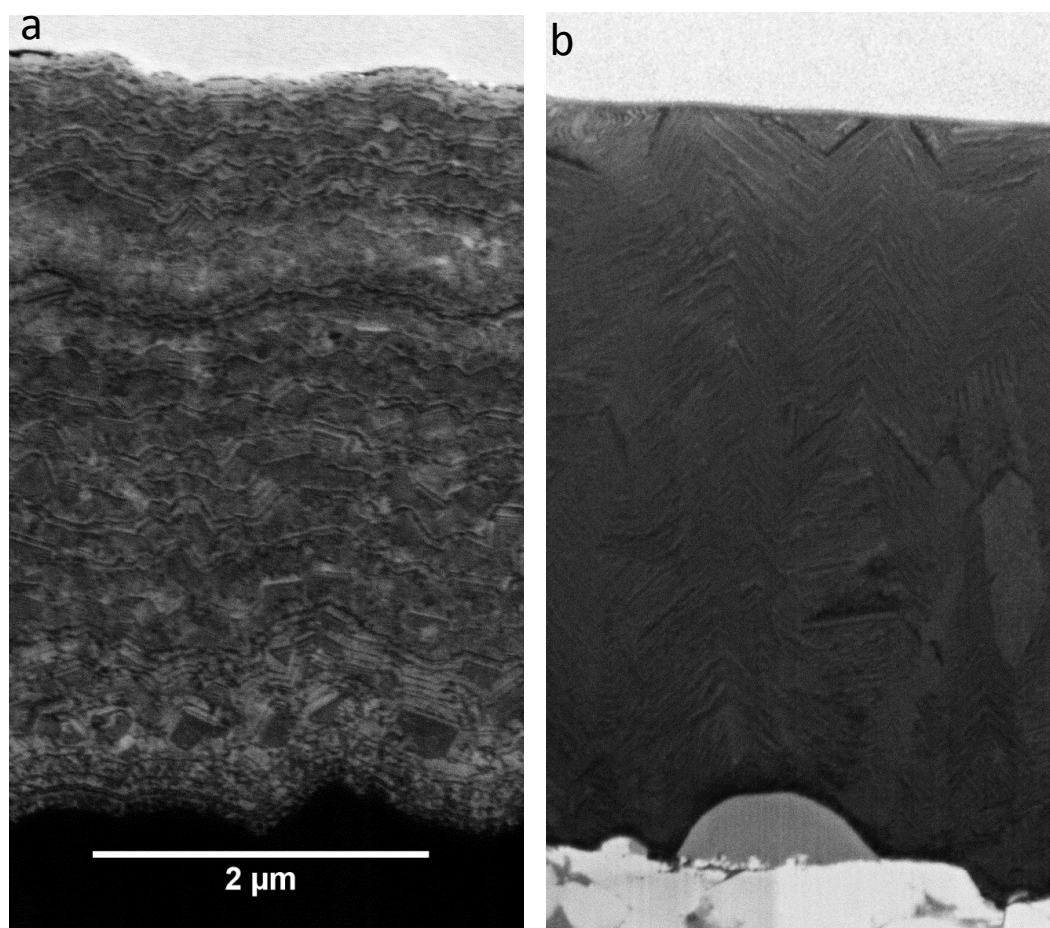
ESI Figure S1 | Cross-sectional microstructure of the hierarchical film. **a**, SEM micrographs of the film's cross-section with 9 hard sublayers and 9 tough interlayers deposited onto a WC-Co substrate coated with a TiN bonding layer and finalized by an AlN top oxidation resistant layer. **b-f**, TEM cross-sectional micrographs showing cube and herringbone crystallites in the thick hard sublayers.



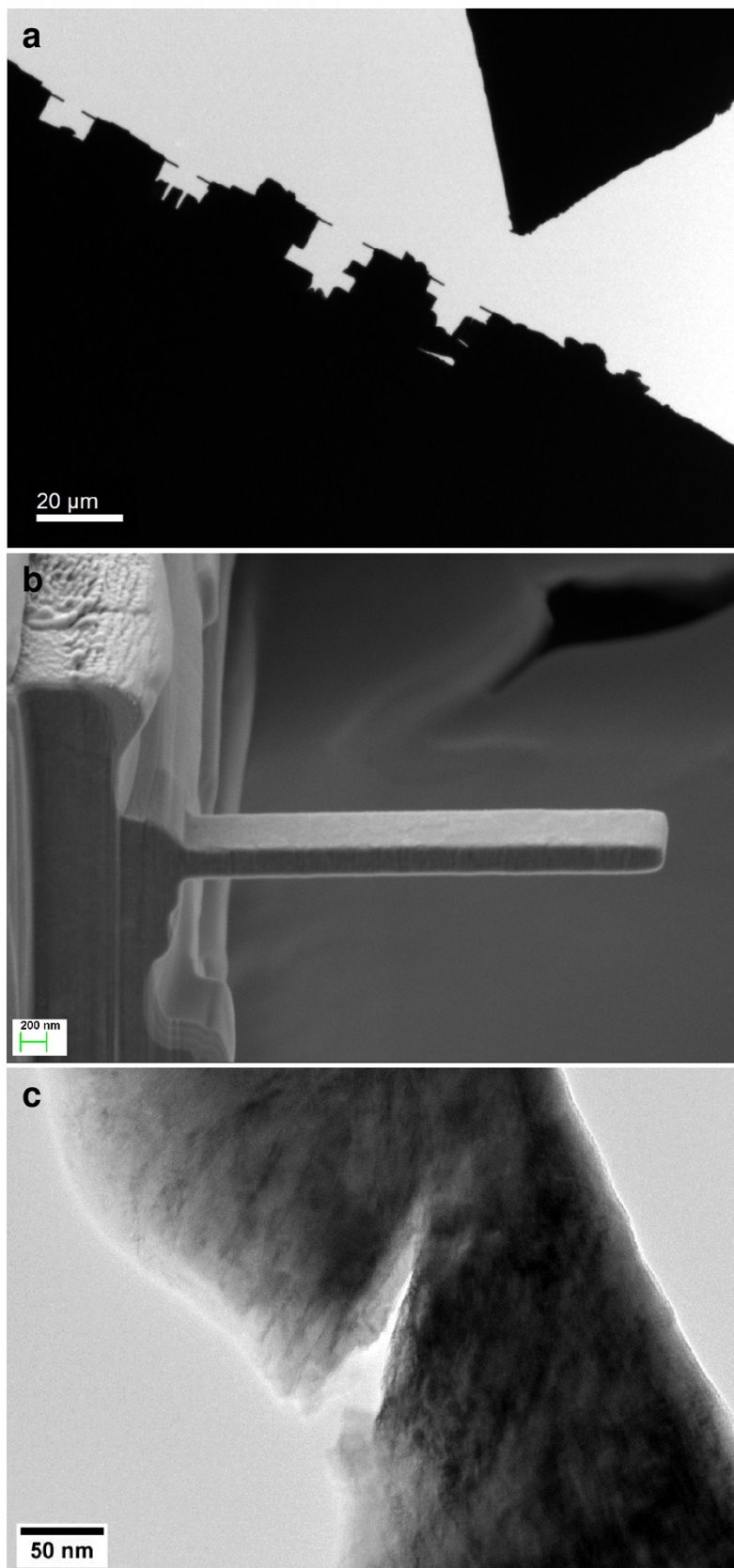
ESI Figure S2 | Atomistic microstructure of micro- and nanocrystals in hard and tough sublayers of the hierarchical film. a, HR-TEM micrograph showing coherent nanolamellae with thin c-Ti(Al)N and thick c-Al(Ti)N platelets in the hard sublayers. **b**, HR-TEM micrograph showing incoherent and partly irregular nanolamellar microstructure of a tough interlayer with thin c-Ti(Al)N platelets (indicated approximately by dotted lines) and thick h-Al(Ti)N platelets of random orientation along with a globular h-Al(Ti)N nanocrystal with its (1210) lattice planes satisfying diffraction condition.



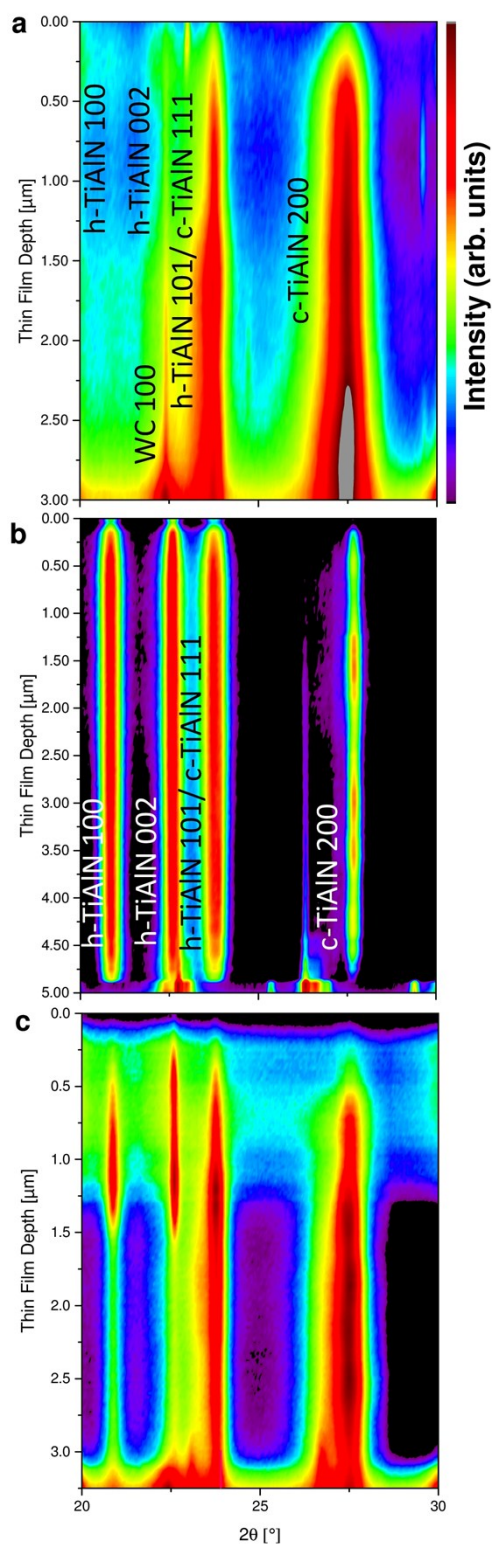
ESI Figure S3 | Cross-sectional microstructure of a microcantilever machined from the hierarchical film. The SEM micrograph shows an irregularly arranged multilayer stack consisting of hard sublayers separated by thin (bright) tough interlayers. The wavy cross-sectional morphology is a result of complex self-organization phenomena and is favorable for the film's fracture properties.



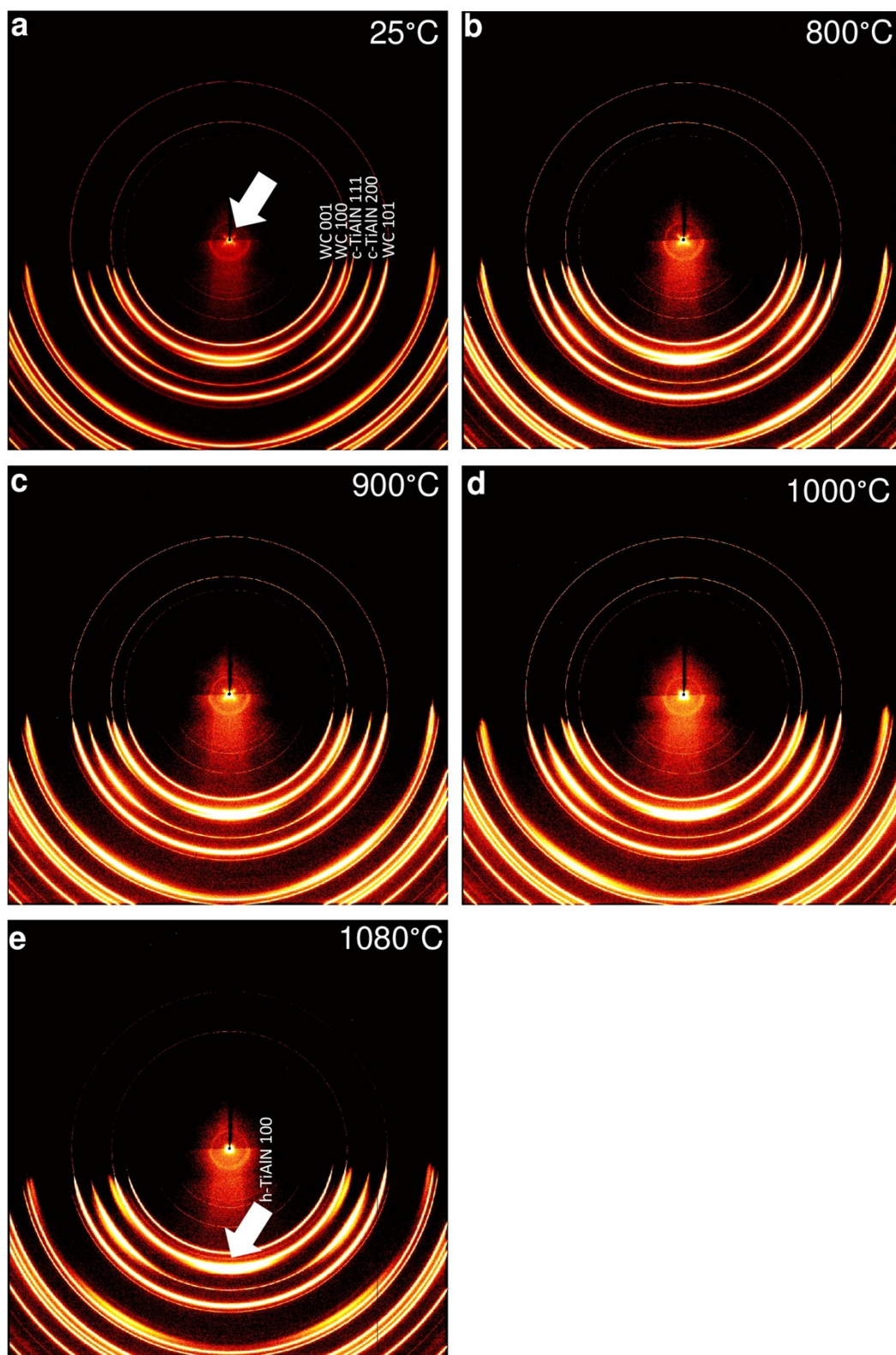
ESI Figure S4 | Cross-sectional microstructure of the reference films. SEM micrographs indicate nanocrystalline (a) and coarse-grained (b) microstructures of the soft and hard reference films, respectively.



ESI Figure S5 | Loading experiments on nanocantilevers in TEM. **a**, A diamond tip approaching the nanocantilevers. **b**, A detailed view of a nanocantilever. **c**, Zigzag-like crack propagation across a nanocantilever machined from the hierarchical film.



ESI Figure S6 | Results from cross-sectional X-ray nanodiffraction analysis (CSnanoXRD) performed on hard, soft and hierarchical films using a synchrotron X-ray beam with a diameter of 100nm and a photon energy of 12.7keV. a, Monolithic hard film consists of cubic TiAlN phases (and also some traces of hexagonal TiAlN phase with concentration < ~5%). **b,** Monolithic soft film consists of hexagonal and cubic TiAlN phases. **c,** Hierarchical film consists of hard and tough sublayers with cubic and hexagonal TiAlN phases. Due to the wavy morphology of the hierarchical film (cf. Extended Data Figure 3), it was not possible to resolve the individual sublayers of the film using CSnanoXRD.



ESI Figure S7 | Results from high-energy high-temperature transmission X-ray diffraction experiment on the hard film on WC-Co substrate demonstrate the film's thermal stability. a-d, Wide angle X-ray diffraction patterns collected at temperatures of 25, 800, 900, 1000 and 1080°C. In patterns **a-c**, only the presence of WC and c-TiAlN diffraction peaks is observed, whereas in **d**, the occurrence of h-TiAlN 100 reflection is visible. The arrow in **a** indicates the small-angle scattering signal from the film's lamellar nanostructure, which disappears in **d** and **e**.